
COUNTERFACTUAL CAUSAL INFERENCE IN NATURAL LANGUAGE WITH LARGE LANGUAGE MODELS

Anonymous authors

Paper under double-blind review

ABSTRACT

Causal structure discovery methods are commonly applied to structured data where the causal variables are known and where statistical testing can be used to assess the causal relationships. By contrast, recovering a causal structure from unstructured natural language data such as news articles contains numerous challenges due to the absence of known variables or counterfactual data to estimate the causal links. Large Language Models (LLMs) have shown promising results in this direction but also exhibit limitations. This work investigates LLM’s abilities to build causal graphs from text documents and perform counterfactual causal inference. We propose an end-to-end causal structure discovery and causal inference method from natural language: we first use an LLM to extract the instantiated causal variables from text data and build a causal graph. We merge causal graphs from multiple data sources to represent the most exhaustive set of causes possible. We then conduct counterfactual inference on the estimated graph. The causal graph conditioning allows reduction of LLM biases and better represents the causal estimands. We use our method to show that the limitations of LLMs in counterfactual causal reasoning come from prediction errors and propose directions to mitigate them. We demonstrate the applicability of our method on real-world news articles.

1 INTRODUCTION

Recovering the causal structure of events described in single or multiple text sources is an important problem for natural language understanding, analysis, and prediction. In particular, causal structure discovery from news articles can help build causal world models that can be used to understand the causal chains behind events, forecast future events, and create robust automated reasoning agents (Schölkopf et al., 2021; Bareinboim et al., 2022). This problem is not often tackled in natural language processing (NLP) because it requires solving multiple challenges considered open research problems in causality and NLP research. First, the text modality prevents the direct use of traditional structure discovery methods as the set of causal variables is not available and has to be discovered (a problem being recently tackled by the field of causal representation learning) (Schölkopf et al., 2021). Second, real-world events have non-trivial structures prone to latent variables and feedback loops, typically excluded from most causal analyses using Direct Acyclic Graphs (DAGs) (Bongers et al., 2021). Third, causal models provide a means to answer interventional and counterfactual queries, but real-world data prevents the ground truth from being directly accessible. This is the *fundamental problem of causal inference* (Pearl, 2009): only one factual world can be observed. In addition, real-world events are often complex and multi-causal, greatly hindering the possibility of manually annotating a ground truth.

Large Language Models (LLMs) have demonstrated impressive abilities to solve tasks related to these problems, notably for understanding and summarising natural language (Devlin et al., 2019; Brown et al., 2020; Bubeck et al., 2023). Recent work (Jiralerspong et al., 2024) has also shown that LLMs can recover causal structures, although the authors do not apply it to text data. However, this ability is still debated as the LLM’s performance can drop significantly when facing unfamiliar settings (Jin et al., 2024). Moreover, while being able to perform some causal reasoning tasks successfully (Melnichuk et al., 2022), notably on commonsense causal reasoning (Kiciman et al., 2023; Zhang et al., 2022), LLMs have shown limitations on tasks that require robust reasoning, such as arithmetic tasks in unfamiliar settings (Wu et al., 2023), or abstract reasoning (Gendron et al., 2024). To explain this behavior difference, (Zecevic et al., 2023) advanced that LLMs cannot discover new

causal relationships but only recall ones already seen during training. Acknowledging this limitation, alternative approaches have been proposed using LLMs to extract causal relationships from text (Rožanec et al., 2023b; Rožanec et al.). However, such approaches do not formally test whether the extracted relationships are causal.

We investigate ways to overcome this restriction and propose an end-to-end causal structure discovery and counterfactual inference method from purely unstructured natural language text data. Our framework is divided into two steps: first, we use an LLM to generate the causal graph associated with a document, i.e., that describes the causal relationships between the events depicted in the text. Optionally, we merge causal graphs from multiple sources using a second LLM. Then, we use the built causal structure to perform an atomic intervention on the sequence of events and infer the consequences in this counterfactual scenario using an LLM (i.e., answer *what if?* questions). We show that our method can effectively extract causal relationships and propose plausible counterfactual worlds from real-world events.

Our contributions can be summarised as follows:

- We propose a method to perform causal structure discovery and counterfactual inference in an end-to-end and explainable way,
- We demonstrate its applicability on real-world events,
- We use our method to disentangle the steps required for counterfactual reasoning and highlight the limitations of LLMs. We show that LLMs can fail even when the full reasoning structure is given and that the bottleneck for performance comes from the prediction step.

Our code is available at this anonymous repository: <https://anonymous.4open.science/r/counterfactual-llm-inference-84BB>

2 RELATED WORK

Causal Structure Discovery with LLMs Text data is often unstructured, high-dimensional, and large-scale. Causal variables may not be directly accessible from the text, and the causal relationships are typically vague and rare, with semantic ambiguity complicating analysis. These challenges greatly hinder the usability of traditional causal structure discovery methods and motivate using LLMs for causal structure discovery (Kiciman et al., 2023; Ma, 2024). (Kiciman et al., 2023) have achieved promising results when using LLMs to infer the causal direction between two variables. Nevertheless, there is some evidence that LLMs, in many cases, repeat embedded causal knowledge (Zecevic et al., 2023) and are susceptible to inferring causal relations from the order of two entities mentioned in a text (Joshi et al., 2024). (Jiralerspong et al., 2024) attempts to recover the full causal structure using a breadth-first search on a set of text variables. (Hobbhahn et al., 2022) investigates whether LLMs can identify the cause and the effect between two natural language sentences. This line of work uses the LLM’s inner knowledge to discover causal relationships between data points. However, recent work highlighted that LLMs do not conduct proper causal reasoning and mainly rely on domain knowledge and correlations (Zecevic et al., 2023; Jin et al., 2024). This approach differs from another line of work that uses the LLM as an information retrieval engine to extract causal relationships explicitly present in the data. For instance, (Gopalakrishnan et al., 2024) uses LLMs to extract causal relationships from medical texts. Our approach combines both worlds as we use an LLM to retrieve causal relationships from text and then perform causal inference on the extracted model to assess the quality of the causal model. NATURAL (Dhawan et al., 2024) is another method developed concurrently to our work using LLMs to perform causal inference. However, the method is based on the Potential Outcome Framework (POF) and computes the Average Treatment Effect (ATE) of a variable (i.e., outcome) under an intervention (i.e., a treatment). By contrast, our method is based on Structural Causal Models (SCMs) and includes a causal structure discovery step to represent complex causal relationships between observed variables. Our work also focuses on counterfactuals, while this method is suited to answer interventional queries.

Strategic Foresight Strategic Foresight aims to provide a structured approach to gathering information regarding plausible future scenarios and adequately preparing for change. It provides expert insights regarding trends and emerging issues that can be considered for strategic planning and policy-making. As such, it is being increasingly adopted in the public and private sectors (Burt & Nair,

2020; Rosa et al., 2021). Among the most frequently used methods, we find scenario planning (Ebadi et al., 2022), which aims to foresee relevant scenarios based on trends and factors of influence to understand better how actions can influence the future (Wilkinson, 2017). While the value of artificial intelligence for strategic foresight has been recognized, much of the work is still not automated (Reez, 2020; Brandtner & Mates, 2021). Scientific literature reports on using artificial intelligence for information scanning and analysis (Parrish et al., 2019; Brandtner & Mates, 2021), to identify weak signals and trends (Geurts et al., 2022), and extract actions and outcomes that can be mapped to causal decision diagrams (Pratt et al., 2023). More recently, authors have proposed architectures that could automate strategic foresight. Nevertheless, the proposed architecture only considered a signal assessment module without explicit reference to testing causality among the extracted graph relationships (Rozanec et al., 2023; Rožanec et al., 2023a). We aim to bridge this gap by identifying, extracting, and testing causal relationships reported in media news to construct a graph of causal relationships and use such a graph to build plausible future scenarios, providing expert insights for strategic planning and policy-making.

3 COUNTERFACTUAL INFERENCE WITH LARGE LANGUAGE MODELS

This section describes our proposed method for causal structure discovery and causal inference from text. We build a modified version of the Structural Causal Model (SCM) (Pearl, 2009) to represent the described causal mechanisms. Following the SCM framework, we consider that the mechanisms can be represented as Directed Acyclic Graphs (DAGs). For every document D , we construct a DAG $\mathcal{G} = \langle \mathbf{U}, \mathbf{V}, \mathbf{E} \rangle$ where the observed nodes $v \in V$ correspond to general depictions of the events in the text. Two nodes $(V_i, V_j) \in \mathbf{V} \times \mathbf{V}$ are connected by an edge $E_{ij} = (V_i, V_j) \in \mathbf{E}$ if a causal relationship between them is explicitly mentioned in the text data (according to an LLM). We also represent possible exogenous factors $U \in \mathbf{U}$ describing unobserved events having a causal influence on the observations. Nodes and edges also have features. Nodes correspond to causal variables and have a *domain* established during extraction and a *current value* from this domain. Confounders U are not assigned values because they are not observed. As we aim to use an LLM for inference, we also keep attributes in plain natural language: a *description* of the variable and additional *contextual information*. Edges also have a *description* attribute. For example, given this sentence: “The airlines companies have seen their revenues diminishing due to travel restrictions.”, we can extract the following causal variables S and T , and their relationship: *travel restrictions* (S) \rightarrow *airlines revenues* (T). Their domains can be, e.g., a boolean for S and a fixed set of categories for T (since we do not have access to the numerical values of the revenues). Their current values are written $S = s_o$ and $T = t_o$. During counterfactual inference, we intervene to modify these values while the other attributes remain unchanged. For performance, we add contextual information to each node, i.e., background knowledge extracted from the text. In this example, the contextual information could be the country where the event takes place. The edge description can be, e.g., “travel restrictions diminish airlines companies revenues”.

SCMs typically have a set of mapping functions \mathcal{F} to infer the value of a variable V given its parents $\text{pa}(\cdot)$ (e.g., $V \leftarrow f_V(\text{pa}(V))$). Instead of using a set of predefined functions, we perform causal inference using an LLM. We also use it to compute the prior probability distribution of the confounders U . We discuss our method and the implications of using an LLM for inference in Section 3.2. We note a full causal model containing the causal graph \mathcal{G} and all these attributes as $\mathcal{M} = \langle \mathcal{G}, \text{LLM} \rangle$. The instantiated model $\mathcal{M}(D)$ describes the model with the values of each variable extracted from the document D . We further note an intervention $do(X = x)$ in this model as $\mathcal{M}_{X=x}(D)$ or $\mathcal{M}(D, do(X = x))$.

Our proposed method is divided into four stages. First, we extract the causal graph from a text document. If multiple documents are provided, we merge their respective causal graphs together. Then, we compute counterfactual worlds from the resulting causal graph. We use these counterfactuals to self-evaluate the causal graph. Section 3.1 describes the causal graph extraction step. Section 3.2 describes the counterfactual inference step. Evaluation is described in Sections 4.3 and 5. Figure 1 illustrates the complete pipeline.

162
163
164
165
166
167
168
169
170
171
172
173
174
175
176
177
178
179
180
181
182
183
184
185
186
187
188
189
190
191
192
193
194
195
196
197
198
199
200
201
202
203
204
205
206
207
208
209
210
211
212
213
214
215

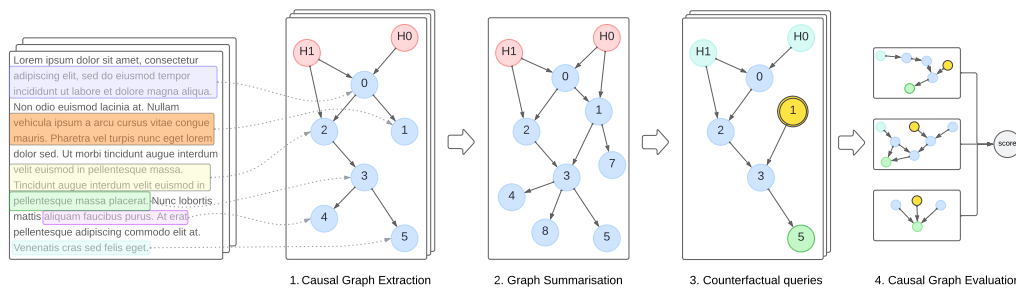


Figure 1: Overview of the proposed framework. (1) An LLM extracts causal variables and their corresponding causal relationships from the input text. (2) Multiple graphs are generated and merged into a single graph if multiple text snippets are given in input. (3) The resulting causal graph is edited using ablation, intervention, and prediction steps to build counterfactual instantiations. The LLM performs inference given the variables’ parent values. (4) The LLM self-evaluates the original and counterfactual graphs.

3.1 CAUSAL STRUCTURE DISCOVERY FROM NATURAL LANGUAGE

We prompt an LLM to read an input document and return its associated causal graph. The expected graph should contain the full set of observed causal variables, their relationships, and their attributes as described in the introduction of Section 3. We also ask the LLM to estimate the hidden variables affecting the observed events and how they are connected. Estimated hidden variables have the same attributes as the observed ones but do not have an observed value. Other works have studied ways to improve the quality of the generated causal graphs, e.g., via breadth-first search (Jiralerspong et al., 2024). However, to keep our pipeline efficient, we only consider a single forward pass with chain-of-thought prompting (Wei et al., 2022). We find that this simple choice is sufficient for our purpose. This is not surprising as the causal relationships to be found are explicitly described in the data and LLMs have been very successful at information retrieval tasks (Brown et al., 2020; Bubeck et al., 2023; Reid et al., 2024). We prompt the LLM to return its answer in JSON format. Still, it may not always provide an extractable response. To alleviate this issue, we allow the LLM to refine its answer several times if it cannot be parsed automatically. If multiple documents are provided, we merge the causal graphs together. We describe this optional step in Appendix A.

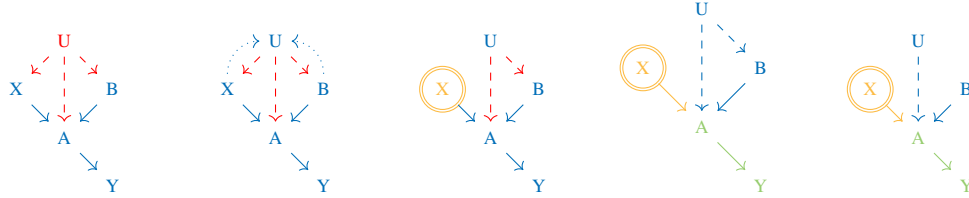
3.2 COUNTERFACTUAL CAUSAL INFERENCE

Autoregressive LLMs are inference engines computing the conditional probability of an output token Y_0 given an input context \mathbf{C} : $P(Y_0|\mathbf{C})$. When used for generation, they construct an output sequence $\mathbf{Y} = [Y_0, \dots, Y_N]$ by computing $P(Y_i|Y_{i-1}, \dots, Y_0, \mathbf{C})$ iteratively. Due to their extensive training on a massive amount of data, LLMs are good estimators of $P(Y_0|\mathbf{C})$ (Brown et al., 2020). However, LLMs are also prone to hallucinations when providing long answers: they deviate from the instructions or state false information (Huang et al., 2023). Indeed, estimating the true conditional distribution of the full output $P(\mathbf{Y}|\mathbf{C})$ is more challenging, especially when \mathbf{Y} is long as it requires building a probability tree considering all possible values for the intermediate Y_i . This tree can be approximated using beam search or heuristic-guided tree search algorithms (Yao et al., 2023; Wan et al., 2024). However, their performance is still dependent on the output length. We alleviate this problem by conditioning the inference query on the causal parents of the output, i.e. instead of providing the complete context \mathbf{C} as an input of the LLM, we use the much smaller subset $\mathbf{pa}(\mathbf{Y}) \subset \mathbf{C}$. Assuming knowledge of the causal graph, this choice can greatly reduce the size of the context window and mitigate hallucination. In the rest of this section, we assume that the LLM can provide a close estimate of the true conditional distribution $P(\mathbf{Y}|\mathbf{pa}(\mathbf{Y}))$. We challenge this assumption in our experiments. We investigate LLMs’ causal inference abilities in counterfactual settings given the estimated causal model \mathcal{M} . Counterfactual queries answer the question: “How would variable Y change if we had $X = x$ instead of $X = x'$?”. This question can be answered by performing *abduction*, *intervention* and *prediction*. The abduction step estimates the values of the exogenous factors U from the observed quantities: $P(U|x', y')$. The intervention step edits the

causal graph with the $do(X = x)$ operation. The prediction step computes the remaining variables from their parent values: $P(Y|\text{pa}(Y))$. The corresponding quantity is expressed as follows:

$$P(Y|do(x), x', y') = \sum_{u \in U} P(Y|do(x), u)P(u|x', y') \quad (1)$$

Figure 2 illustrates these steps. To be efficient, we approximate some of them. We sample a single $u \sim P(U|\text{ch}(U))$ using the LLM. $\text{ch}(\cdot)$ represents the children of U . We perform the abduction and prediction steps only on the variables affected by the intervention, as shown in Figure 2e where we use the LLM as described above to compute $P(A|X, B, U)$ and $P(Y|A)$.



(a) Factual graph. (b) Abduction step. (c) Intervention step. (d) Prediction step. (e) Optimised version.

Figure 2: Counterfactual inference steps. (2a) The original causal graph. (2b) We estimate the possible values of the exogenous factors, here U , from the observations. (2c) We perform the $do(X = x)$ operation. (2d) We predict the values of the remaining variables given their parent causes. Here, X and U are known. B , A and Y should be predicted. (2e) However, to maintain efficiency, we consider a single possible value per exogenous factor and re-compute only the variables affected by the intervention: here B is unaffected and not re-computed.

4 INFERENCE ON SYNTHETIC DATA

4.1 EXPERIMENTAL SETUP

We verify the applicability of our method on synthetic data and use it to investigate the current limitations of LLMs on counterfactual reasoning tasks. Cladder is a synthetic dataset containing small self-contained causal graphs of three or four variables with no unobserved confounders (Jin et al., 2023). Queries in Cladder test the causal capabilities of a model. We focus on the counterfactual subset. We extract the results for the counterfactuals queries (rung 3, det-counterfactual)¹. Queries are divided into commonsense, nonsensical and anti-commonsense categories. Nonsensical queries are composed of abstract variables not conveying any semantic meaning. Anti-commonsense queries contain common concepts as variables but with fictive causal relationships. Figure 3 shows an example of anti-commonsense query from Cladder. We conduct experiments using LLaMA-3.1 (Dubey et al., 2024), GPT-3.5 (Ouyang et al., 2022), GPT-4 (version 1106), GPT-4o and GPT-4o-mini (OpenAI, 2023; 2024). We query GPT models via the OpenAI API while we run LLaMA-3.1 locally on one GPU NVIDIA A100 using Ollama. We use Langchain to interface with the LLMs. We use the default hyperparameters of both models and allow 12 refinement steps to format the LLM answers properly. When the answer does not match the expected format, we add a parsing layer. The prompts used are given in Appendix B. Our framework is denoted *Counterfactual-CI*. We compare our method with baseline LLM models from (Jin et al., 2023).

4.2 EVALUATION RESULTS

We compare the results using our framework against basic and causal prompting (Jin et al., 2023). To provide insights into the abilities and limitations of LLMs, we also create ablated models. These models, denoted with \mathcal{G}_{gt} are provided with the ground-truth graph (extracted by parsing the input query) and are only tasked to perform the counterfactual inference step. Table 1 describes the obtained

¹We download the results divided by query type and commonsense here: <https://edmond.mpg.de/dataset.xhtml?persistentId=doi%3A10.17617%2F3.NVRRRA9>.

270
271
272
273
274
275
276
277
278
279
280
281
282
283
284
285
286
287
288
289
290
291
292
293
294
295
296
297
298
299
300
301
302
303
304
305
306
307
308
309
310
311
312
313
314
315
316
317
318
319
320
321
322
323

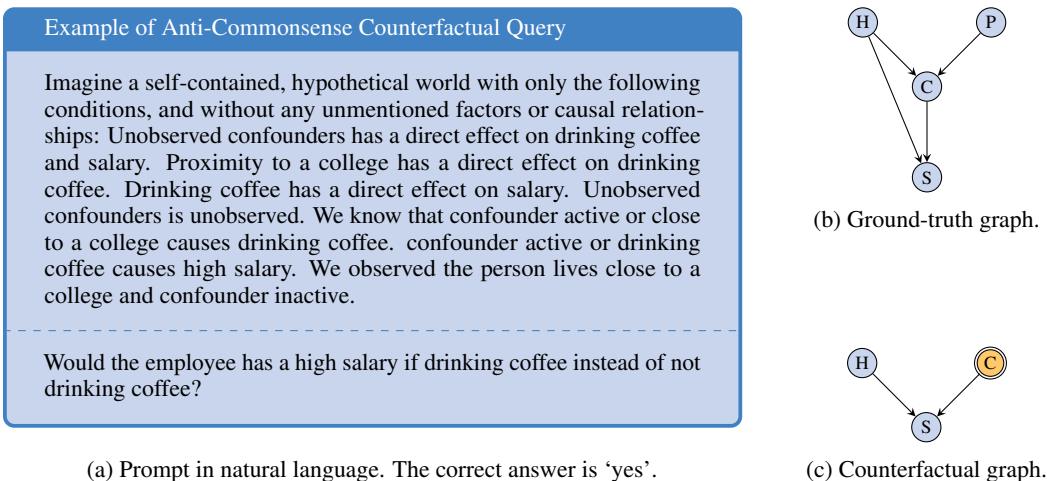


Figure 3: Example of counterfactual query from the Cladder dataset. (left) The context and question description in natural language as provided to the model. (right) The corresponding ground-truth and counterfactual causal graph with (H) a hidden confounder, unlike in real-world situations, its value is given in the dataset and thus shown in blue, (C) coffee drinking, and (S) a high or low salary. All causes affecting the system are mentioned. Intervention is shown in yellow.

results. We do not include parsing errors in the computation of the results as we aim to study the abilities of the LLMs on causal inference tasks separately from their capacity to follow instructions and generate structured outputs. This is not an issue for most models as they only contain a small number of uniformly distributed errors (see Figure 4). Most LLMs do not perform significantly better than random guessing (50% accuracy). There is no consistent difference of accuracy between the three levels of commonsense, showing little bias towards prior knowledge. The best models are GPT-4-1106+Causal CoT and Counterfactual-CI-GPT-4o- \mathcal{G}_{gt} although their performance remains limited (around 10% better than random guessing). Our framework decomposes counterfactual reasoning into a sequence of atomic steps, allowing us to get insights into the LLMs’ causal reasoning abilities. We observe an improvement of performance when the causal graph is given to the LLM. This is most noticeable with GPT-4o. It indicates that LLMs are not systematically able to recover the true causal structure even when no information is hidden. However, the improvements are often small, e.g. no improvement is observed for GPT-3.5, highlighting that the accuracy seldom depends on the access to the correct causal structure. Our framework ensures that the right causal factors are provided to the appropriate causal variables, i.e. the value of a variable is solely determined by the value of its parents or from an intervention. Therefore, the bottleneck in accuracy lies in the computation of the functions $P(\mathbf{Y}|\text{pa}(\mathbf{Y}))$. We provide an example of failure case illustrating this limitation in LLMs in Section 4.4.

We look deeper into Figure 4 and Table 2. Figure 4 shows the decomposition of the results between graph building and inference errors. Table 2 further shows the Graph Edit Distances (GED) between the causal graphs built by the models and the ground-truth causal graphs. The GED counts the number of node and edge edits required to transform the first graph to the second. We can see in Figure 4 that most LLMs can accurately build a causal graph. Only LLaMA-3.1 shows a high number of errors during the causal graph generation. Moreover, Table 2 shows that GPT-4o, GPT-4o-mini and GPT-3.5 require less than one modification in average to recover the true graph (GED metric). As the $\text{GED}_{\text{topology}}$ metric is very close to the GED, it indicates that a semantic difference is systematically associated with a structural difference. This is further confirmed by the observed difference between the $\text{GED}_{\text{topology}}$ and $\text{IoU-GED}_{\text{topology}}$ metrics.

4.3 LLM SELF-EVALUATION

We ask the LLM to self-evaluate its generated factual and counterfactual graphs. Each sample in the dataset contains a context document a query. Thus, one factual graph corresponding to the context and a second counterfactual graph with the intervention are generated for each sample. We summarise

Table 1: Accuracy on the counterfactual subset of the Cladder dataset. Only extracted answers are shown. Accuracy is reported overall and divided by commonsense (Common.), nonsensical and anticommonsense (Anti-Common) queries. Models with \mathcal{G}_{gt} are given the true causal graph extracted via standard parsing. Results with * are obtained on $\sim 65\%$ of the dataset and cannot be directly compared with the other models (see Figure 4). LLMs do not demonstrate good counterfactual inference abilities even when the causal and reasoning structures are given, highlighting that the performance bottleneck lies in the LLMs’ ability to perform accurate prediction.

	Accuracy			
	Overall	Common.	Nonsensical	Anti-Common.
LLaMA	56.61	54.99	58.26	54.78
GPT-3 Non-Instr. (davinci)	50.00	47.01	49.17	47.78
GPT-3 Instr. (text-davinci-001)	50.07	53.28	50.82	45.22
GPT-3 Instr. (text-davinci-002)	51.76	54.13	51.93	48.99
GPT-3 Instr. (text-davinci-003)	58.02	54.13	59.23	59.42
GPT-3.5	50.49	51.85	51.38	47.25
GPT-4-1106	59.77	61.25	59.78	58.26
GPT-4-1106 + CausalCoT	62.31	63.53	60.06	65.78
Counterfactual-CI-GPT-4-1106*	50.57	51.17	49.33	52.94
-GPT-4o	52.26	53.85	51.39	52.37
-GPT-4o-mini	51.86	54.19	51.22	50.80
-GPT-3.5	52.31	48.39	53.57	53.92
-LLaMA-3.1*	52.11	53.00	53.11	48.39
-GPT-4o- \mathcal{G}_{gt}	60.53	58.68	61.23	61.20
-GPT-4o-mini- \mathcal{G}_{gt}	56.58	53.16	58.03	56.91
-GPT-3.5- \mathcal{G}_{gt}	49.80	47.78	48.41	54.52
-LLaMA-3.1- \mathcal{G}_{gt}	58.05	54.33	61.17	54.79

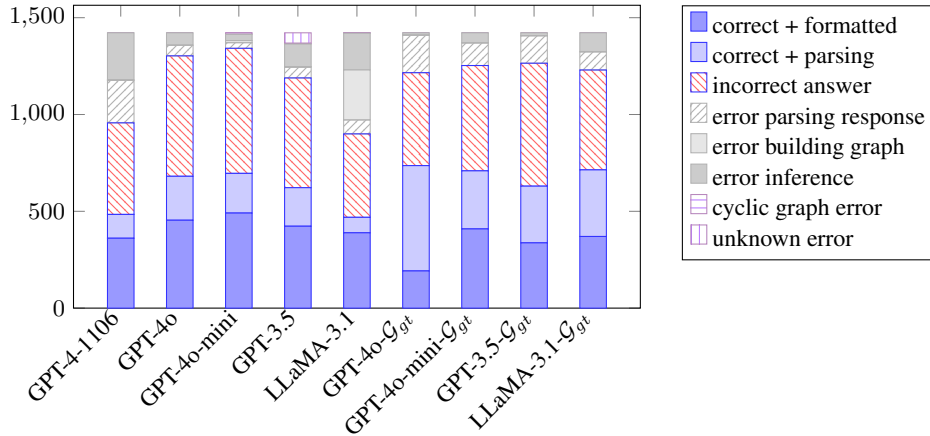


Figure 4: Partition of the Counterfactual-CI models results between correct, incorrect answers and errors. Errors in grey are not considered as counterfactual reasoning errors but as instruction errors and are not considered in the results of Table 1. Models can usually generate the causal structure and conduct inference. GPT-4-1106 and LLaMA-3.1 show a lower capacity to follow instructions and generate structured outputs. Models also often require to have their response parsed to extract the answer, particularly GPT-4o- \mathcal{G}_{gt} .

each graph into text format and prompt the LLM to return a plausibility score for the chain of events and a confidence score for its prediction (prompts are given in Appendix B.4). Table 3 shows the average LLM self-evaluation on the accuracy of the generated causal graphs. The models expectedly attribute a slightly lower plausibility to the counterfactual graphs. Models attributing a higher score also show a higher confidence. In addition, the models that obtain a higher accuracy in Table 1 tend to attribute lower scores and confidence than their counterparts. We put these results in perspective with the evaluation on real-world graphs in Section 5.

Table 2: Graph distances with ground-truth graph. GED stands for Graph Edit Distance. IoU-GED is the GED metric between the intersection and the union of the built and ground-truth graphs. The base metric matches the variable names while the topology metric only look at the structure. All graphs have either three and four nodes. Most models require less than one change in average, except for GPT-4o-mini and LLaMA-3.1.

	GED	IoU-DEG	GED _{topology}	IoU-GED _{topology}
Counterfactual-CI-GPT-4-1106	0.814	3.929	0.814	2.240
-GPT-4o	0.897	4.268	0.897	2.100
-GPT-4o-mini	2.667	5.898	2.666	6.175
-GPT-3.5	0.582	3.708	0.579	0.919
-LLaMA-3.1	2.420	6.198	2.419	4.790

Table 3: Self-evaluation and confidence provided by the LLMs. Results for GPT-3.5 are omitted because the model did not return properly formatted scores on a sufficient number of samples (less than five). Models attribute a slightly lower score to the counterfactual graphs. Models performing better tend to attribute lower scores and confidence than their counterparts.

	Self-Evaluation		Self-Confidence	
	Factual	Counterfactual	Factual	Counterfactual
GPT-4-1106	0.689	0.650	0.899	0.907
GPT-4o	0.506	0.489	0.666	0.707
GPT-4o-mini	0.501	0.452	0.732	0.722
GPT-3.5	-	-	-	-
LLaMA-3.1	0.772	0.764	0.820	0.829

4.4 EXAMPLE OF REASONING FAILURES

We show an example of failure case with GPT-4o for the example provided in Figure 3. The model explanation is given below:

The target variable 'salary' is influenced by two parent causes: 'drinking coffee' and 'unobserved confounders'. Given that the person drinks coffee (true), we might expect the salary to be positively affected. However, the status of unobserved confounders is inactive, which suggests a lack of additional income influence. Thus, the overall effect results in a low salary.

Although the model generates the correct causal factual and counterfactual graphs (as shown in the figure), the inference step fails. The model answers 'low salary' instead of 'high salary'. The context specifies that 'confounder active or drinking coffee causes high salary' but the LLM makes a mistake and interprets it as a logical AND instead of a logical OR. This example illustrates the type of prediction error that is prevalent in the LLMs' reasoning. It can be compared with the LLM limitations in robust and abstract reasoning tasks (Wu et al., 2023; Gendron et al., 2024; Jin et al., 2024).

5 EXPERIMENTS ON REAL-WORLD USECASE

5.1 EXPERIMENTAL SETUP

We extract 5,486 media events related to the "Price of Oil" from EventRegistry (Leban et al., 2014). These events, spanning the first quarters of 2015, 2020, 2022, and 2023, were selected based on geopolitical events highlighted by the U.S. Energy Information Administration and the Russo-Ukrainian War ². We perform experiments using LLaMA-3.1 (Dubey et al., 2024) and GPT-4o (OpenAI, 2023; 2024). We provide early results on real-world news documents. Due to the unavailability of the ground truth, we focus our experiments on a handful of documents that we manually verify.

²The geopolitical events were highlighted in the following report, last accessed on August 25th 2023: https://www.eia.gov/finance/markets/crudeoil/spot_prices.php.

432 5.2 COUNTERFACTUAL INFERENCE
 433
 434

435 Table 4: Example of counterfactual inference performed by the Counterfactual-CI model on real-
 436 world data. The first row shows the extracted factual graph and the counterfactual graph under
 437 interventions (in yellow) $do(0='low')$ and $do(9='False')$. The exogenous factor is in red. After
 438 abduction, a value is assigned to it (illustrated in blue). Variables inferred during the prediction step
 439 are shown in green. The bottom rows show the values of the factual and counterfactual worlds.

Factual Graph		Intervened Graph	
Factual Values		Counterfactual Values	
		GPT-4o	LLaMA-3.1
0	Severity of COVID-19 pandemic (range element): severe	low (from do operation)	
1	Severity of oil price war (range element): severe		
2	Bursa Malaysia downtrend magnitude (int): 29%	20	high
3	FBM KLCI index value (float): 1,280.63	1580	1500.00
4	Selling pressure on stocks (range element): high		
5	Investors moving into cash (bool): True		
9	Malaysia's change of coalition government (bool): True	False (from do operation)	
10	Downside risks to corporate earnings (range element): high	low	low
11	Travel restrictions imposed worldwide (range element): severe	none	none
12	Condition of oil & gas and airlines sectors (range element): bad	good	good
h0	Potential end of COVID-19 pandemic (bool): None	False	True

461
 462 Table 4 provides an example of results obtained with our method for a model $\mathcal{M}(D)$ extracted from
 463 a document D and under interventions $\mathcal{M}_{0='low',9='False'}(D)$. The input text and the explanations
 464 given by the LLMs during inference are given in Appendix C. The document D describes how
 465 the COVID-19 pandemic and the rise in oil prices affect Malaysia's economy. We perform two
 466 interventions on the graph and build a counterfactual world where the severity of the pandemic is low
 467 and a change of government has not happened. From these interventions, the model updates the rest
 468 of the variables and predicts a better economical situation. We emphasise that these results should be
 469 taken as an illustrative example only. We also observe that the two models return different values for
 470 the exogenous factor but reach the same conclusions.

471 As in Section 4.3, we ask the LLM to self-evaluate its generated graphs. We generate four causal
 472 graphs from a single document and, for each graph, we automatically build six counterfactual queries.
 473 We summarise each graph into text format and prompt the LLM to return a plausibility score for the
 474 chain of events and a confidence score for its prediction (prompts are given in Appendix B.4). We
 475 show the results in Table 5. The LLMs generally provide higher scores to the factual graph than to the
 476 counterfactuals. This is not surprising as the former are extracted from real data, closer to the LLMs'
 477 training distribution. However, they still give high scores to the built counterfactuals. GPT-4o is
 478 also more consistent on the factual graphs, with a lower standard deviation, highlighting consistency
 479 between graph generations. LLaMA-3.1 shows a high standard deviation for all results.

480 GPT-4o gives higher scores and confidence than on the synthetic data despite the more complex
 481 causal structure. However, LLaMA-3.1 provides lower scores, particularly for the counterfactual
 482 graph. We hypothesise that lower scores are attributed to the counterfactual graphs because they
 483 break the causal reasoning chains via the intervention. It hints that the LLMs rely on commonsense
 484 clues and already observed reasoning chains from their training distribution to build their answers.
 485 This can be further observed in the explanations provided in Appendix B.4 and was described in the
 context of abstract reasoning by (Gendron et al., 2024).

Table 5: Self-evaluation and confidence provided by the LLMs on the plausibility of the described set of events and their causal relationships for the document described in Appendix B. The average of three end-to-end runs is shown.

	Self-Evaluation		Self-Confidence	
	Factual	Counterfactuals	Factual	Counterfactuals
Counterfactual-CI-GPT-4o	0.850 \pm 0.000	0.739 \pm 0.129	0.863 \pm 0.022	0.762 \pm 0.155
-LLaMA-3.1	0.563 \pm 0.330	0.256 \pm 0.340	0.600 \pm 0.346	0.367 \pm 0.400

6 LIMITATIONS

LLMs provide free-text answers that can be different from the format provided in the instructions. This poses challenges for building an end-to-end pipeline that requires using LLMs at multiple stages, as the responses can be difficult to parse automatically, and errors can accumulate. In our future work, we will include fine-tuning in our pipeline to mitigate this issue. Due to the high cost of running LLMs or accessing them through APIs, we only tested our method on synthetic data and short text snippets. We intend to apply it to larger amounts of data in the future. We also only consider DAG structures, whereas real-world events can contain feedback loops. We will integrate them into our future work. As the LLM discovers the causal structure, errors can be present, and confounders can be omitted. The counterfactual results depend on the causal graph to be accurate. In addition, our current approach for real-world data proxies ground-truth counterfactual data by retrieving such values from LLMs. Our future work will focus on verifying the accuracy of the intermediate steps and building ground-truth counterfactual data.

7 CONCLUSION AND BROADER IMPACT

We propose an end-to-end method for conducting causal structure discovery and counterfactual causal inference from unstructured natural language. We demonstrate the applicability of our method on real-world news events, showcasing the LLMs’ abilities to perform causal discovery and inference not as a standalone model but as a part of a larger framework. Furthermore, our experiments show that LLMs can extract the causal structure of a piece of text but fail during the reasoning part. This expands previous findings on the limitations of LLMs on reasoning tasks (Wu et al., 2023; Gendron et al., 2024; Jin et al., 2024).

This research is still in its infancy but has shown promising results for computing causal inference and leveraging LLMs. As the inference process is divided into several independent computations of causal variables given their parents, this configuration provides inherent interpretability and allows auditing an LLM’s answer. Our future work will follow two lines of research. On one hand, as LLMs have been shown to perform better by using refinement techniques (Wu et al., 2023; Madaan et al., 2023; Yuan et al., 2024; Qiu et al., 2024), our counterfactual self-evaluation method could be used to conduct *Counterfactual Self-Learning*: refine LLMs’ answers to improve them and teach LLMs to reason more causally by providing them with counterfactual data (Bareinboim et al., 2022). On the other hand, we aim to create a framework to build and test counterfactuals based on real values and validate whether LLM-extracted causal relationships hold. Doing so would avoid LLM hallucinations and counterfactual reasoning deficiencies similar to the ones shown in Section 4 and lead to robust causal reasoning, where every piece of information could be traced back to evidence from the real world. We expect that such a framework will have extensive applications in many domains, extending the use of causal reasoning to any domain where text is available. In particular, we expect that could lead to a greater automation of strategic foresight, democratizing and enabling a wider use of it to enhance decision-making at all societal levels.

REFERENCES

Elias Bareinboim, Juan D. Correa, Duligur Ibeling, and Thomas Icard. On pearl’s hierarchy and the foundations of causal inference. In Hector Geffner, Rina Dechter, and Joseph Y. Halpern (eds.), *Probabilistic and Causal Inference: The Works of Judea Pearl*, volume 36 of *ACM Books*, pp.

540 507–556. ACM, 2022. doi: 10.1145/3501714.3501743. URL [https://doi.org/10.1145/](https://doi.org/10.1145/3501714.3501743)
541 3501714.3501743.

542

543 Stephan Bongers, Patrick Forré, Jonas Peters, and Joris M. Mooij. Foundations of structural causal
544 models with cycles and latent variables. *The Annals of Statistics*, 49(5):2885 – 2915, 2021. doi:
545 10.1214/21-AOS2064. URL <https://doi.org/10.1214/21-AOS2064>.

546 Patrick Brandtner and Marius Mates. Artificial intelligence in strategic foresight—current practices
547 and future application potentials: Current practices and future application potentials. In *The 2021*
548 *12th International Conference on E-business, Management and Economics*, pp. 75–81, 2021.

549

550 Tom B. Brown, Benjamin Mann, Nick Ryder, Melanie Subbiah, Jared Kaplan, Prafulla Dhari-
551 wal, Arvind Neelakantan, Pranav Shyam, Girish Sastry, Amanda Askell, Sandhini Agar-
552 wal, Ariel Herbert-Voss, Gretchen Krueger, Tom Henighan, Rewon Child, Aditya Ramesh,
553 Daniel M. Ziegler, Jeffrey Wu, Clemens Winter, Christopher Hesse, Mark Chen, Eric Sigler,
554 Mateusz Litwin, Scott Gray, Benjamin Chess, Jack Clark, Christopher Berner, Sam McCand-
555 lish, Alec Radford, Ilya Sutskever, and Dario Amodei. Language models are few-shot
556 learners. In Hugo Larochelle, Marc’Aurelio Ranzato, Raia Hadsell, Maria-Florina Balcan,
557 and Hsuan-Tien Lin (eds.), *Advances in Neural Information Processing Systems 33: Annual*
558 *Conference on Neural Information Processing Systems 2020, NeurIPS 2020, December 6-12,*
559 *2020, virtual*, 2020. URL [https://proceedings.neurips.cc/paper/2020/hash/](https://proceedings.neurips.cc/paper/2020/hash/1457c0d6bfc4967418bfb8ac142f64a-Abstract.html)
560 1457c0d6bfc4967418bfb8ac142f64a-Abstract.html.

561 Sébastien Bubeck, Varun Chandrasekaran, Ronen Eldan, Johannes Gehrke, Eric Horvitz, Ece Kamar,
562 Peter Lee, Yin Tat Lee, Yuanzhi Li, Scott M. Lundberg, Harsha Nori, Hamid Palangi, Marco Túlio
563 Ribeiro, and Yi Zhang. Sparks of artificial general intelligence: Early experiments with GPT-4.
564 *CoRR*, abs/2303.12712, 2023. doi: 10.48550/arXiv.2303.12712. URL [https://doi.org/10.](https://doi.org/10.48550/arXiv.2303.12712)
565 48550/arXiv.2303.12712.

566 George Burt and Anup Karath Nair. Rigidities of imagination in scenario planning: Strategic foresight
567 through ‘unlearning’. *Technological Forecasting and Social Change*, 153:119927, 2020.

568

569 Jacob Devlin, Ming-Wei Chang, Kenton Lee, and Kristina Toutanova. BERT: pre-training of
570 deep bidirectional transformers for language understanding. In Jill Burstein, Christy Doran, and
571 Tamar Solorio (eds.), *Proceedings of the 2019 Conference of the North American Chapter of*
572 *the Association for Computational Linguistics: Human Language Technologies, NAACL-HLT*
573 *2019, Minneapolis, MN, USA, June 2-7, 2019, Volume 1 (Long and Short Papers)*, pp. 4171–
574 4186. Association for Computational Linguistics, 2019. doi: 10.18653/v1/N19-1423. URL
575 <https://doi.org/10.18653/v1/n19-1423>.

576

577 Nikita Dhawan, Leonardo Cotta, Karen Ullrich, Rahul G. Krishnan, and Chris J. Maddison. End-to-
578 end causal effect estimation from unstructured natural language data. *CoRR*, abs/2407.07018, 2024.
579 doi: 10.48550/ARXIV.2407.07018. URL [https://doi.org/10.48550/arXiv.2407.](https://doi.org/10.48550/arXiv.2407.07018)
580 07018.

581 Abhimanyu Dubey, Abhinav Jauhri, Abhinav Pandey, Abhishek Kadian, Ahmad Al-Dahle, Aiesha
582 Letman, Akhil Mathur, Alan Schelten, Amy Yang, Angela Fan, Anirudh Goyal, Anthony Hartshorn,
583 Aobo Yang, Archi Mitra, Archie Sravankumar, Artem Korenev, Arthur Hinsvark, Arun Rao, Aston
584 Zhang, Aurélien Rodriguez, Austen Gregerson, Ava Spataru, Baptiste Rozière, Bethany Biron,
585 Binh Tang, Bobbie Chern, Charlotte Caucheteux, Chaya Nayak, Chloe Bi, Chris Marra, Chris
586 McConnell, Christian Keller, Christophe Touret, Chunyang Wu, Corinne Wong, Cristian Canton
587 Ferrer, Cyrus Nikolaidis, Damien Allonsius, Daniel Song, Danielle Pintz, Danny Livshits, David
588 Esiobu, Dhruv Choudhary, Dhruv Mahajan, Diego Garcia-Olano, Diego Perino, Dieuwke Hupkes,
589 Egor Lakomkin, Ehab AlBadawy, Elina Lobanova, Emily Dinan, Eric Michael Smith, Filip
590 Radenovic, Frank Zhang, Gabriel Synnaeve, Gabrielle Lee, Georgia Lewis Anderson, Graeme
591 Nail, Grégoire Mialon, Guan Pang, Guillem Cucurell, Hailey Nguyen, Hannah Korevaar, Hu Xu,
592 Hugo Touvron, Iliyan Zarov, Imanol Arrieta Ibarra, Isabel M. Kloumann, Ishan Misra, Ivan
593 Evtimov, Jade Copet, Jaewon Lee, Jan Geffert, Jana Vranes, Jason Park, Jay Mahadeokar, Jeet
594 Shah, Jelmer van der Linde, Jennifer Billock, Jenny Hong, Jenya Lee, Jeremy Fu, Jianfeng
595 Chi, Jianyu Huang, Jiawen Liu, Jie Wang, Jiecao Yu, Joanna Bitton, Joe Spisak, Jongsoo Park,
596 Joseph Rocca, Joshua Johnstun, Joshua Saxe, Junteng Jia, Kalyan Vasuden Alwala, Kartikeya

594 Upasani, Kate Plawiak, Ke Li, Kenneth Heafield, Kevin Stone, and et al. The llama 3 herd
595 of models. *CoRR*, abs/2407.21783, 2024. doi: 10.48550/ARXIV.2407.21783. URL <https://doi.org/10.48550/arXiv.2407.21783>.
596
597

598 Ashkan Ebadi, Alain Auger, and Yvan Gauthier. Detecting emerging technologies and their evolution
599 using deep learning and weak signal analysis. *Journal of Informetrics*, 16(4):101344, 2022.
600

601 Martin Ester, Hans-Peter Kriegel, Jörg Sander, Xiaowei Xu, et al. A density-based algorithm for
602 discovering clusters in large spatial databases with noise. In *kdd*, volume 96, pp. 226–231, 1996.
603

604 Kenneth D. Forbus. Analogical abduction and prediction: Their impact on deception. In *2015 AAAI
605 Fall Symposia, Arlington, Virginia, USA, November 12-14, 2015*, pp. 15–20. AAAI Press, 2015.
606 URL <http://www.aaai.org/ocs/index.php/FSS/FSS15/paper/view/11660>.
607

608 Gaël Gendron, Qiming Bao, Michael Witbrock, and Gillian Dobbie. Large language models are not
609 strong abstract reasoners. In Kate Larson (ed.), *Proceedings of the Thirty-Third International Joint
610 Conference on Artificial Intelligence, IJCAI-24*, pp. 6270–6278. International Joint Conferences
611 on Artificial Intelligence Organization, 8 2024. doi: 10.24963/ijcai.2024/693. URL <https://doi.org/10.24963/ijcai.2024/693>. Main Track.
612

613 Amber Geurts, Ralph Gutknecht, Philine Warnke, Arjen Goetheer, Elna Schirrmeister, Babette
614 Bakker, and Svetlana Meissner. New perspectives for data-supported foresight: The hybrid
615 ai-expert approach. *Futures & Foresight Science*, 4(1):e99, 2022.
616

617 Seethalakshmi Gopalakrishnan, Luciana Garbayo, and Wlodek Zadrozny. Causality extraction from
618 medical text using large language models (llms). *arXiv preprint arXiv:2407.10020*, 2024.
619

620 Luigi Gresele, Julius von Kügelgen, Jonas M. Kübler, Elke Kirschbaum, Bernhard Schölkopf,
621 and Dominik Janzing. Causal inference through the structural causal marginal problem. In
622 Kamalika Chaudhuri, Stefanie Jegelka, Le Song, Csaba Szepesvári, Gang Niu, and Sivan Sabato
623 (eds.), *International Conference on Machine Learning, ICML 2022, 17-23 July 2022, Baltimore,
624 Maryland, USA*, volume 162 of *Proceedings of Machine Learning Research*, pp. 7793–7824.
625 PMLR, 2022. URL <https://proceedings.mlr.press/v162/gresele22a.html>.
626

627 Marius Hobbhahn, Tom Lieberum, and David Seiler. Investigating causal understanding in llms. In
628 *NeurIPS ML Safety Workshop*, 2022.
629

630 Lei Huang, Weijiang Yu, Weitao Ma, Weihong Zhong, Zhangyin Feng, Haotian Wang, Qianglong
631 Chen, Weihua Peng, Xiaocheng Feng, Bing Qin, and Ting Liu. A survey on hallucination in large
632 language models: Principles, taxonomy, challenges, and open questions. *CoRR*, abs/2311.05232,
633 2023. doi: 10.48550/ARXIV.2311.05232. URL [https://doi.org/10.48550/arXiv.
634 2311.05232](https://doi.org/10.48550/arXiv.2311.05232).
635

636 Zhijing Jin, Yuen Chen, Felix Leeb, Luigi Gresele, Ojasv Kamal, Zhiheng Lyu, Kevin Blin, Fer-
637 nando Gonzalez Adauto, Max Kleiman-Weiner, Mrinmaya Sachan, and Bernhard Schölkopf.
638 Cladder: A benchmark to assess causal reasoning capabilities of language models. In Alice Oh,
639 Tristan Naumann, Amir Globerson, Kate Saenko, Moritz Hardt, and Sergey Levine (eds.),
640 *Advances in Neural Information Processing Systems 36: Annual Conference on Neural
641 Information Processing Systems 2023, NeurIPS 2023, New Orleans, LA, USA, December 10 -
642 16, 2023*, 2023. URL [http://papers.nips.cc/paper_files/paper/2023/hash/
643 631bb9434d718ea309af82566347d607-Abstract-Conference.html](http://papers.nips.cc/paper_files/paper/2023/hash/631bb9434d718ea309af82566347d607-Abstract-Conference.html).
644

645 Zhijing Jin, Jiarui Liu, Zhiheng Lyu, Spencer Poff, Mrinmaya Sachan, Rada Mihalcea, Mona T.
646 Diab, and Bernhard Schölkopf. Can large language models infer causation from correlation? In
647 *The Twelfth International Conference on Learning Representations, ICLR 2024, Vienna, Austria,
648 May 7-11, 2024*. OpenReview.net, 2024. URL [https://openreview.net/forum?id=
649 vqIH00bdqL](https://openreview.net/forum?id=vqIH00bdqL).
650

651 Thomas Jiralerspong, Xiaoyin Chen, Yash More, Vedant Shah, and Yoshua Bengio. Efficient causal
652 graph discovery using large language models. *CoRR*, abs/2402.01207, 2024. doi: 10.48550/
653 ARXIV.2402.01207. URL <https://doi.org/10.48550/arXiv.2402.01207>.
654

648 Nitish Joshi, Abulhair Saparov, Yixin Wang, and He He. Llms are prone to fallacies in causal
649 inference. *arXiv preprint arXiv:2406.12158*, 2024.

650

651 Emre Kiciman, Robert Ness, Amit Sharma, and Chenhao Tan. Causal reasoning and large language
652 models: Opening a new frontier for causality. *CoRR*, abs/2305.00050, 2023. doi: 10.48550/arXiv.
653 2305.00050. URL <https://doi.org/10.48550/arXiv.2305.00050>.

654 Thomas N. Kipf and Max Welling. Semi-supervised classification with graph convolutional networks.
655 In *5th International Conference on Learning Representations, ICLR 2017, Toulon, France, April 24-*
656 *26, 2017, Conference Track Proceedings*. OpenReview.net, 2017. URL [https://openreview.](https://openreview.net/forum?id=SJU4ayYgl)
657 [net/forum?id=SJU4ayYgl](https://openreview.net/forum?id=SJU4ayYgl).

658 Gregor Leban, Blaz Fortuna, Janez Brank, and Marko Grobelnik. Event registry: learning about
659 world events from news. In *Proceedings of the 23rd International Conference on World Wide Web*,
660 pp. 107–110, 2014.

661

662 Jing Ma. Causal inference with large language model: A survey. *arXiv preprint arXiv:2409.09822*,
663 2024.

664 Aman Madaan, Niket Tandon, Prakhar Gupta, Skyler Hallinan, Luyu Gao, Sarah Wiegrefe, Uri
665 Alon, Nouha Dziri, Shrimai Prabhunoye, Yiming Yang, Sean Welleck, Bodhisattwa Prasad
666 Majumder, Shashank Gupta, Amir Yazdanbakhsh, and Peter Clark. Self-refine: Iterative refinement
667 with self-feedback. *CoRR*, abs/2303.17651, 2023. doi: 10.48550/arXiv.2303.17651. URL
668 <https://doi.org/10.48550/arXiv.2303.17651>.

669 Valentyn Melnychuk, Dennis Frauen, and Stefan Feuerriegel. Causal transformer for estimating
670 counterfactual outcomes. In Kamalika Chaudhuri, Stefanie Jegelka, Le Song, Csaba Szepesvári,
671 Gang Niu, and Sivan Sabato (eds.), *International Conference on Machine Learning, ICML 2022,*
672 *17-23 July 2022, Baltimore, Maryland, USA*, volume 162 of *Proceedings of Machine Learning*
673 *Research*, pp. 15293–15329. PMLR, 2022. URL <https://proceedings.mlr.press/v162/melnychuk22a.html>.

674

675 OpenAI. GPT-4 technical report. *CoRR*, abs/2303.08774, 2023. doi: 10.48550/ARXIV.2303.08774.
676 URL <https://doi.org/10.48550/arXiv.2303.08774>.

677

678 OpenAI. Hello gpt-4o, 2024. URL <https://openai.com/index/hello-gpt-4o/>. Ac-
679 cessed: 2024-09-23.

680 Matías Osta-Vélez and Peter Gärdenfors. Analogy as a search procedure: a dimensional view. *Journal*
681 *of Experimental & Theoretical Artificial Intelligence*, 0(0):1–20, 2022. doi: 10.1080/0952813X.
682 2022.2125081. URL <https://doi.org/10.1080/0952813X.2022.2125081>.

683

684 Long Ouyang, Jeffrey Wu, Xu Jiang, Diogo Almeida, Carroll L. Wainwright, Pamela Mishkin,
685 Chong Zhang, Sandhini Agarwal, Katarina Slama, Alex Ray, John Schulman, Jacob Hilton, Fraser
686 Kelton, Luke Miller, Maddie Simens, Amanda Askell, Peter Welinder, Paul F. Christiano, Jan
687 Leike, and Ryan Lowe. Training language models to follow instructions with human feedback.
688 In Sanmi Koyejo, S. Mohamed, A. Agarwal, Danielle Belgrave, K. Cho, and A. Oh (eds.),
689 *Advances in Neural Information Processing Systems 35: Annual Conference on Neural Information*
690 *Processing Systems 2022, NeurIPS 2022, New Orleans, LA, USA, November 28 - December*
691 *9, 2022*, 2022. URL [http://papers.nips.cc/paper_files/paper/2022/hash/](http://papers.nips.cc/paper_files/paper/2022/hash/b1efde53be364a73914f58805a001731-Abstract-Conference.html)
[b1efde53be364a73914f58805a001731-Abstract-Conference.html](http://papers.nips.cc/paper_files/paper/2022/hash/b1efde53be364a73914f58805a001731-Abstract-Conference.html).

692

693 Nathan H Parrish, Anna L Buczak, Jared T Zook, James P Howard, Brian J Ellison, and Benjamin D
694 Baugher. Crystal cube: Multidisciplinary approach to disruptive events prediction. In *Advances in*
695 *Human Factors, Business Management and Society: Proceedings of the AHFE 2018 International*
696 *Conference on Human Factors, Business Management and Society, July 21-25, 2018, Loews*
Sapphire Falls Resort at Universal Studios, Orlando, Florida, USA 9, pp. 571–581. Springer, 2019.

697

698 Judea Pearl. *Causality*. Cambridge university press, 2 edition, 2009. doi: 10.1017/
699 CBO9780511803161.

700

701 Lorien Pratt, Christophe Bisson, and Thierry Warin. Bringing advanced technology to strategic
decision-making: The decision intelligence/data science (di/ds) integration framework. *Futures*,
152:103217, 2023.

-
- 702 Linlu Qiu, Liwei Jiang, Ximing Lu, Melanie Sclar, Valentina Pyatkin, Chandra Bhagavatula, Bailin
703 Wang, Yoon Kim, Yejin Choi, Nouha Dziri, and Xiang Ren. Phenomenal yet puzzling: Testing
704 inductive reasoning capabilities of language models with hypothesis refinement. In *The Twelfth In-*
705 *ternational Conference on Learning Representations, ICLR 2024, Vienna, Austria, May 7-11, 2024.*
706 OpenReview.net, 2024. URL <https://openreview.net/forum?id=bNt7oaJl2a>.
707
- 708 Norbert Reez. Foresight-based leadership. decision-making in a growing ai environment. In *Intern-*
709 *ational Security Management: New Solutions to Complexity*, pp. 323–341. Springer, 2020.
- 710 Machel Reid, Nikolay Savinov, Denis Teplyashin, Dmitry Lepikhin, Timothy P. Lillicrap, Jean-
711 Baptiste Alayrac, Radu Soricut, Angeliki Lazaridou, Orhan Firat, Julian Schrittwieser, Ioannis
712 Antonoglou, Rohan Anil, Sebastian Borgeaud, Andrew M. Dai, Katie Millican, Ethan Dyer,
713 Mia Glaese, Thibault Sottiaux, Benjamin Lee, Fabio Viola, Malcolm Reynolds, Yuanzhong Xu,
714 James Molloy, Jilin Chen, Michael Isard, Paul Barham, Tom Hennigan, Ross McIlroy, Melvin
715 Johnson, Johan Schalkwyk, Eli Collins, Eliza Rutherford, Erica Moreira, Kareem Ayoub, Megha
716 Goel, Clemens Meyer, Gregory Thornton, Zhen Yang, Henryk Michalewski, Zaheer Abbas,
717 Nathan Schucher, Ankesh Anand, Richard Ives, James Keeling, Karel Lenc, Salem Haykal,
718 Siamak Shakeri, Pranav Shyam, Aakanksha Chowdhery, Roman Ring, Stephen Spencer, Eren
719 Sezener, and et al. Gemini 1.5: Unlocking multimodal understanding across millions of tokens
720 of context. *CoRR*, abs/2403.05530, 2024. doi: 10.48550/ARXIV.2403.05530. URL <https://doi.org/10.48550/arXiv.2403.05530>.
721
- 722 Aaron B Rosa, Niklas Gudowsky, and Petteri Repo. Sensemaking and lens-shaping: Identifying
723 citizen contributions to foresight through comparative topic modelling. *Futures*, 129:102733, 2021.
724
- 725 Jose Rozanec, Beno Šircelj, Michael Cochez, and Gregor Leban. Back to the future: predicting
726 causal relationships influencing oil prices. In *The Second Tiny Papers Track at ICLR 2024*.
727
- 728 Joze Rozanec, Peter Nemeč, Gregor Leban, and Marko Grobelnik. Ai, what does the future hold
729 for us? automating strategic foresight. In *Companion of the 2023 ACM/SPEC International*
730 *Conference on Performance Engineering*, pp. 247–248, 2023.
- 731 Jože M Rožanec, Radu Prodan, Dumitru Roman, Gregor Leban, and Marko Grobelnik. Ai-based
732 strategic foresight for environment protection. In *Symposium on AI, Data and Digitalization*
733 *(SAIDD 2023)*, volume 7, 2023a.
- 734 Jože M Rožanec, Beno Šircelj, Peter Nemeč, Gregor Leban, and Dunja Mladenčić. Building a causality
735 graph for strategic foresight. 2023b.
736
- 737 Bernhard Schölkopf, Francesco Locatello, Stefan Bauer, Nan Rosemary Ke, Nal Kalchbrenner,
738 Anirudh Goyal, and Yoshua Bengio. Toward causal representation learning. *Proc. IEEE*, 109(5):
739 612–634, 2021. doi: 10.1109/JPROC.2021.3058954. URL <https://doi.org/10.1109/JPROC.2021.3058954>.
740
- 741 Petar Velickovic, Guillem Cucurull, Arantxa Casanova, Adriana Romero, Pietro Liò, and Yoshua
742 Bengio. Graph attention networks. In *6th International Conference on Learning Representations,*
743 *ICLR 2018, Vancouver, BC, Canada, April 30 - May 3, 2018, Conference Track Proceedings.*
744 OpenReview.net, 2018. URL <https://openreview.net/forum?id=rJXmpikCZ>.
745
- 746 Ziyu Wan, Xidong Feng, Muning Wen, Stephen Marcus McAleer, Ying Wen, Weinan Zhang, and Jun
747 Wang. Alphazero-like tree-search can guide large language model decoding and training. In *Forty-*
748 *first International Conference on Machine Learning, ICML 2024, Vienna, Austria, July 21-27, 2024.*
749 OpenReview.net, 2024. URL <https://openreview.net/forum?id=C4OpREezgj>.
750
- 751 Jason Wei, Xuezhi Wang, Dale Schuurmans, Maarten Bosma, Brian Ichter, Fei Xia, Ed H. Chi, Quoc V.
752 Le, and Denny Zhou. Chain-of-thought prompting elicits reasoning in large language models. In
753 *NeurIPS*, 2022. URL http://papers.nips.cc/paper_files/paper/2022/hash/9d5609613524ecf4f15af0f7b31abca4-Abstract-Conference.html.
754
- 755 Angela Wilkinson. Strategic foresight primer. *European Political Strategy Centre*, 2017.

756 Zhaofeng Wu, Linlu Qiu, Alexis Ross, Ekin Akyürek, Boyuan Chen, Bailin Wang, Najoung Kim,
757 Jacob Andreas, and Yoon Kim. Reasoning or reciting? exploring the capabilities and limitations of
758 language models through counterfactual tasks. *CoRR*, abs/2307.02477, 2023. doi: 10.48550/arXiv.
759 2307.02477. URL <https://doi.org/10.48550/arXiv.2307.02477>.
760

761 Keyulu Xu, Weihua Hu, Jure Leskovec, and Stefanie Jegelka. How powerful are graph neural
762 networks? In *7th International Conference on Learning Representations, ICLR 2019, New Orleans,
763 LA, USA, May 6-9, 2019*. OpenReview.net, 2019. URL [https://openreview.net/forum?
764 id=ryGs6iA5Km](https://openreview.net/forum?id=ryGs6iA5Km).

765 Shunyu Yao, Dian Yu, Jeffrey Zhao, Izhak Shafran, Tom Griffiths, Yuan Cao, and Karthik
766 Narasimhan. Tree of thoughts: Deliberate problem solving with large language models. In
767 Alice Oh, Tristan Naumann, Amir Globerson, Kate Saenko, Moritz Hardt, and Sergey Levine
768 (eds.), *Advances in Neural Information Processing Systems 36: Annual Conference on Neural
769 Information Processing Systems 2023, NeurIPS 2023, New Orleans, LA, USA, December 10 -
770 16, 2023*, 2023. URL [http://papers.nips.cc/paper_files/paper/2023/hash/
771 271db9922b8d1f4dd7aaef84ed5ac703-Abstract-Conference.html](http://papers.nips.cc/paper_files/paper/2023/hash/271db9922b8d1f4dd7aaef84ed5ac703-Abstract-Conference.html).

772 Weizhe Yuan, Richard Yuanzhe Pang, Kyunghyun Cho, Sainbayar Sukhbaatar, Jing Xu, and Jason
773 Weston. Self-rewarding language models. *CoRR*, abs/2401.10020, 2024. doi: 10.48550/ARXIV.
774 2401.10020. URL <https://doi.org/10.48550/arXiv.2401.10020>.
775

776 Matej Zecevic, Moritz Willig, Devendra Singh Dhami, and Kristian Kersting. Causal parrots: Large
777 language models may talk causality but are not causal. *Trans. Mach. Learn. Res.*, 2023, 2023.
778 URL <https://openreview.net/forum?id=tv46tCzs83>.

779 Jiayao Zhang, Hongming Zhang, Weijie J. Su, and Dan Roth. ROCK: causal inference principles
780 for reasoning about commonsense causality. In *International Conference on Machine Learning,
781 ICML 2022, 17-23 July 2022, Baltimore, Maryland, USA*, volume 162 of *Proceedings of Machine
782 Learning Research*, pp. 26750–26771. PMLR, 2022. URL [https://proceedings.mlr.
783 press/v162/zhang22am.html](https://proceedings.mlr.press/v162/zhang22am.html).
784
785
786
787
788
789
790
791
792
793
794
795
796
797
798
799
800
801
802
803
804
805
806
807
808
809

A GRAPH SUMMARISATION

When considering several documents, we build their corresponding causal graphs independently and then attempt to merge them. The problem of combining multiple causal graphs together is known as the *Structural Causal Marginal problem* (Gresele et al., 2022). This is a challenging problem that we approach from two different angles. Considering two causal models \mathcal{M}_1 and \mathcal{M}_2 , we first generate embeddings for every node of the two graphs by extracting their representation generated by the last hidden layer of the LLM. The prompt of a node is a concatenation of all its attributes. We omit its current value because we want to generate a representation of the variable and not the current instance. Motivated by the success of Graph Neural Networks (GNNs) at aggregating neighborhood information in graphs (Kipf & Welling, 2017; Velickovic et al., 2018; Xu et al., 2019), we also add to the prompt the attributes of its immediate neighbours and how they are connected via the edge attributes. Then, we use a clustering algorithm to find nodes that share similar latent representations. We select DBSCAN (Ester et al., 1996). Since it is a density-based algorithm, it allows us to restrict the sparsity of the clusters and cluster together nodes with only very close representations.

After extracting similar nodes, we consider two ways to combine graphs: *summarisation* and *analogy*. Summarisation implies considering similar nodes as a single node in the merged graph, inheriting the edges of all the nodes in the set. This approach is straightforward and allows reducing the number of nodes as the graph grows. However, assessing if two causal variables can be merged is a challenging problem. In particular, in the absence of a lot of observations (one text only shows one observation per variable), the merged causal graph can be easily falsified (Gresele et al., 2022).

Analogy merging is inspired by the research on analogical reasoning (Osta-Vélez & Gärdenfors, 2022; Forbus, 2015). We view similarity between nodes representations as an indication that analog mechanisms are causing them. To represent an analogy, we do not modify the existing graphs but add a common unobserved ancestor between similar nodes to integrate the similarity information from the clustering process without making assumptions regarding the nature of their similarity. The merged graphs can share information via backdoor paths. Unlike summarisation, analogy does not remove nodes but adds more. However, this method does not introduce ways to falsify the graphs and preserve the mechanisms of the initial graphs. The two approaches are illustrated in Figure 5.

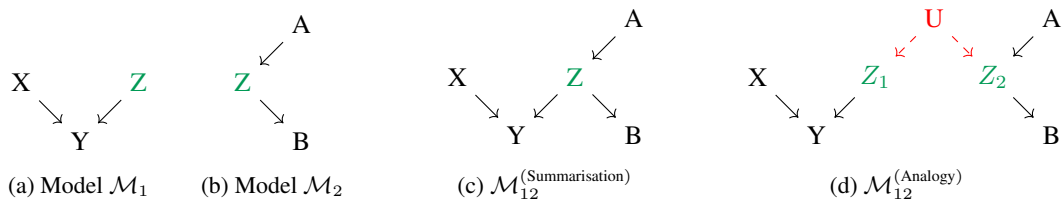


Figure 5: Illustration of graph merging process for two models \mathcal{M}_1 and \mathcal{M}_2 . We assume that the common variable Z is the same in the two graphs and should be combined. Figure 5c shows the merged graph using summarisation: Z is shared by the two mechanisms. Figure 5d shows the merged graph using analogy: the variables Z_1 and Z_2 from \mathcal{M}_1 and \mathcal{M}_2 remain separated but share a common ancestor.

B PROMPTS USED

B.1 CAUSAL STRUCTURE DISCOVERY

Here is the system prompt used for causal discovery:

```
Your task is to summarise a text into a JSON dictionary of instantiated causal variables and
the causal relationships between them.
Variables should be as atomic and detailed as possible. Causal relationships should describe
how the value of the first variable affects the value of the second.
One sentence usually describes two or more variables and connects them. For each variable, the
following questions should be answered:
'What are the causes of this variable's value? Is it fully explained by the available
information or are some causes missing?'
If some causes seem to be missing, create new (hidden) variables.
```

864
865
866
867
868
869
870
871
872
873
874
875
876
877
878
879
880
881
882
883
884
885
886
887
888
889
890
891
892
893
894
895
896
897
898
899
900
901
902
903
904
905
906
907
908
909
910
911
912
913
914
915
916
917

```
Hidden variables represent missing information to fully explain the value of one or more
observed variables.
They cannot have incoming edges. Identify the major and minor variables and how they are
connected.
Add the missing unknown variables when necessary. Follow carefully the instructions and write
down your answer using only the given JSON format very strictly.
The format is as follows:
{
  "observed_nodes": [
    {
      "node_id": (str) "0",
      "description": (str) "<high-level short atomic description of causal variable 0>",
      "type": (str) "<variable type: e.g. bool, int, set element, range element>",
      "values": (str) "<set of possible values, if applicable>",
      "current_value": (str) "<current value>",
      "context": (str) "<contextual information type> : <value of the contextual information
        linked to the current instance>"
    },
    ...
  ],
  "hidden_nodes": [
    {
      "node_id": (str) "h0",
      "description": (str) "<high-level short atomic description of the hidden causal variable
        >",
      "type": (str) "<variable type: e.g. bool, int, set element, range element>",
      "values": (str) "<set of possible values, if applicable>",
      "current_value": (str) "", # This field is left empty because the current value of the
        variable is unknown since the variable is hidden
      "context": (str) "<contextual information type> : <value of the contextual information
        linked to the current instance>"
    },
    ...
  ],
  "observed_edges": [
    {
      "source_node_id": (str) "0",
      "target_node_id": (str) "1",
      "description": (str) "<high-level short atomic description of the causal relationship from
        variable 0 to 1>",
      "details": (str) "<detailed explanation of how the value of variable 0 affects the value
        of variable 1 in the text>"
    },
    ...
  ],
  "hidden_edges": [
    {
      "source_node_id": (str) "h0",
      "target_node_id": (str) "1",
      "description": (str) "<high-level short atomic description of the causal relationship from
        hidden variable 0 to 1>",
      "details": (str) "<detailed explanation of how the value of hidden variable 0 affects the
        value of variable 1 in the text>"
    },
    ...
  ]
}
```

Here is the parameterised user prompt, specific for each instance. The {text} parameter is replaced by the input document.

```
Here is the input text:
...
{text}
...
```

B.2 GRAPH SUMMARISATION

When conducting graph summarisation, we do not use the LLM as a generative model but as an embedding model. We only provide node information using the following format. Texts in curly brackets represent variable parameters.

```
description: {description}, type: {type}, values: {values}, context: {context}
```

918 When adding neighbour information, we concatenate the initial representation with the following
919 neighbour representation:
920

```
921 neighbour at distance {rank} from node: description: {description}, type: {type}, values: {  
922 values}, context: {context}
```

923

924 B.3 COUNTERFACTUAL INFERENCE

925

926 During inference, we provide parent variables to the LLM and prompt it to estimate the value of the
927 target variable. Here is the system prompt:

```
928 Your task is to predict the value of the target variable given its description, type, possible  
929 values, and context, and the attributes and values of its parent causes and the  
930 relationships connecting them.  
931 The value of the target variable is fully determined by its direct list of causes. Reason step-  
932 by-step. Start by describing the attributes of the target variable and explain in your  
933 own words its relationships with its parent causes, how the variables are linked, and how  
934 their values cause the value of the target. Then, predict the value of the target  
variable. Provide a confidence score as a float between 0 and 1. Follow strictly the  
provided format.
```

935

936 The user prompt provides information about the target variable. The format is as follows:

```
937 The target variable has the following attributes: {node attributes}.  
938 It is caused by the following variables:
```

939

940 The list of parent is then provided. The i th parent variable is described as follows:

```
941 {i}. {parent attributes}. Its value is {parent value}. Its causal relationship with the target  
942 is described as follows: {edge attributes}
```

943

944 We generate the value of the intervened variable using an LLM. Here is the system prompt provided
945 for this task:

```
946 Your task is to interpret the attributes of a variable and propose an alternative/  
947 counterfactual instantiation different from its current value. The variable is described  
948 by its description, type, possible values, current value, and context. The counterfactual  
949 value should be a plausible alternative instantiation of the variable given the context,  
950 type, description, and possible values. Reason step-by-step. Start by describing the  
951 attributes of the variable and explain in your own words the reasons for the choice of  
952 the counterfactual value. Then, state the factual value and propose the new  
counterfactual value. Provide a confidence score as a float between 0 and 1. Follow  
strictly the provided format.
```

953

954 Here is the user prompt:

```
955 The variable has the following attributes: description: {description}, type: {type}, possible  
956 values: {values}, context: {context}. The current value is {current_value}. Propose a  
957 counterfactual value.
```

958

959 B.4 EVALUATION

960

961 The evaluation of the causal factual and counterfactual models is performed by an LLM using the
962 following prompts. Here is the system prompt:

```
963 Your task is to evaluate the plausibility of a set of events linked by causal relationships.  
964 The events are described by a high-level description and a value. The events are linked  
965 by causal relationships. The causal relationships are described by a high-level  
966 description. The overall plausibility of the set of events corresponds to the  
967 factorization of the plausibility of each event's occurrence given its causes. Reason  
968 step-by-step. Start by describing the events and the causal relationships. Explain in  
969 your own words the reasons for the plausibility of each event. Finally, provide an  
overall score for the plausibility of the sequence of events. Give an explanation  
describing your reasoning. Provide an overall confidence score as a float between 0 and 1.  
Follow strictly the provided format.
```

970

971 The user prompt describes the events in the topological order of the causal graph. Before each event,
the causal relationships with its parents is also described. Here is an example:

972
973
974
975
976
977
978
979
980
981
982
983
984
985
986
987
988
989
990
991
992
993
994
995
996
997
998
999
1000
1001
1002
1003
1004
1005
1006
1007
1008
1009
1010
1011
1012
1013
1014
1015
1016
1017
1018
1019
1020
1021
1022
1023
1024
1025

```
The causal graph is composed of the following events:  
(parent rank) -> (target rank) (edge description).  
(target rank). (target description). The value is (node current_value)
```

C SUPPLEMENT TO THE EXPERIMENTS

In this section, we describe in more details the counterfactual causal inference example from Table 4. The document from which is extracted the causal graph is shown below:

KUALA LUMPUR: Bursa Malaysia downtrend could be far from over as there is always more room to decline depending on the severity of COVID-19 pandemic and oil price war, said economists after key benchmark FBM KLCI took another beating in the early trading session yesterday.

To what may be seen as continued selling pressure from last week's Friday the 13th, the FTSE Bursa Malaysia KLCI (FBM KLCI) lost 44.99 points to 1,299.76 at 9.10am yesterday, compared with Friday's close of 1,344.75, after opening 25.38 points lower at 1,319.37 yesterday morning.

At market closing yesterday, the FBM KLCI closed at 4.77 per cent lower to 1,280.63 points with turnover at 4.473 billion shares valued at RM3.687 billion.

Bank Islam chief economist Dr Mohd Afzanizam Abdul Rashid said if history is of any guide, the FBM KLCI has fallen sharply between January 11, 2008 (1,516.22 points) and October 29, 2009 (829.41 points).

He said during the Asia Financial Crisis in 1997/1998, the FBM KLCI was down massively by 79.2 per cent between February 25, 1997 (1,265.01 points) and September 1, 1998 (262.7 points).

"For now, the FBM KLCI touches its peak at 1,895.18 points on April 19, 2018 and has plunged by 29.0 per cent to 1,344.75 points as of March 13, 2020. There is always more room to decline obviously due to the virus outbreak and oil price war," he told NST Business.

CGS-CIMB analyst Ivy Ng Lee Fang said the research firm has cut its year-end FBM KLCI target to 1,449 points.

"We advise investors to seek shelter in defensive and high-dividend-yield stocks until the concerns over the global spread of COVID-19 subside.

"These, together with Malaysia's unexpected change of coalition government, could pose downside risks to corporate earnings, which are difficult to measure at this time," it said.

Ng said during the global financial crisis, FBM KLCI fell by 45 per cent from its peak to 829 points, its lowest ever and FBM KLCI earnings fell by 8.7 per cent in 2009.

She said there is a potential earning downside risk of 10.3 per cent to its current 1.6 per cent FBM KLCI earnings per share growth forecast if the earnings risk resembles that of during the global financial crisis decline (-8.7 per cent).

Meanwhile, AxiCorp market strategist Stephen Innes said small and medium enterprises (SMEs) are most at risk given they generally operate on small operating cushions and will need to dive into credit lines if not hefty interest credit card to keep things afloat.

"Unless governments actually get money physically into the hands that need it the most things can turn bad. This will put pressure on bank stocks due to credit line drawdown and an increase in defaults.

"We know oil and gas and airlines are in a bad way due to travel restrictions imposed around the world.

"At this stage, I see no way out and expect more investors to move into cash or keep investment portfolio very light primarily in recessionary proof areas like healthcare.

"But honestly with credit under duress, I think cash is the place to be. The only endgame in sight is when the world sees COVID-19 ends," he said.

Table 6 provides the explanations given by the models when inferring the values of the remaining variables during the prediction step. We can observe that the two models reason similarly, although GPT-4o tends to return a more precise and detailed explanation. The only difference in behaviour is for variable $h0$ where GPT-4o does not answer. As this value is computed during the abduction step, in an anticausal fashion (predict a cause from its consequences), this is expected. This issue can be alleviated by marginalising over the set of possible values of $h0$.

Tables 7 and 8 provide examples of explanation returned by the models when evaluating the factual and counterfactual causal graphs. GPT-4o provides longer and more detailed explanations while the justification provided by LLaMA-3.1 is not always very explanative. We can see that scores and confidence are highly correlated for both models although outliers can also be observed.

1026
1027
1028
1029
1030
1031
1032
1033
1034
1035
1036
1037
1038
1039
1040
1041
1042
1043
1044
1045
1046
1047
1048
1049
1050
1051
1052
1053
1054
1055
1056
1057
1058
1059
1060
1061
1062
1063
1064
1065
1066
1067
1068
1069
1070
1071
1072
1073
1074
1075
1076
1077
1078
1079

Table 6: Explanation of the inferred values by GPT-4o and LLaMA-3.1 for every variable in Table 4.

	GPT-4o	LLaMA-3.1
2	The Bursa Malaysia downtrend magnitude is influenced by several factors. The severity of the COVID-19 pandemic is low, which would typically suggest a smaller downtrend magnitude. However, the severity of the oil price war is severe, which greatly increases the downtrend magnitude. The downside risks to corporate earnings are low, which would also typically suggest a smaller downtrend. Lastly, the potential end of the COVID-19 pandemic is not expected (False), which does not help reduce the downtrend magnitude. Thus, considering the severe impact of the oil price war, I predict a moderate downtrend magnitude of around 20%.	Given that Severity of oil price war is severe, increasing Bursa Malaysia downtrend magnitude and Downside risks to corporate earnings are low, contributing less to the downtrend. Although Potential end of COVID-19 pandemic would reduce the downtrend magnitude, Severity of COVID-19 pandemic being low would increase it, but this effect is expected to be lower than that of oil price war. Hence Bursa Malaysia downtrend magnitude is predicted to be high.
3	The FBM KLCI index value is influenced by several factors for the market close yesterday. The Bursa Malaysia downtrend magnitude shows a significant percentage decline from peak (20%), which has a negative impact on the index. Furthermore, the selling pressure on stocks is high, which also decreases the index value. On the other hand, the condition of the oil & gas and airlines sectors is good, which supports the index value. Given these mixed factors, the FBM KLCI index is estimated to be lower but not drastically so.	The estimated value of the FBM KLCI index is 1500.00 due to the high Bursa Malaysia downtrend magnitude and high selling pressure on stocks, which both decrease the FBM KLCI index value. However, the good condition of oil & gas and airlines sectors has a positive effect on the index value.
10	The downside risks to corporate earnings are influenced by Malaysia’s change of coalition government. Since the change of coalition government did not occur (value is False), the downside risks are expected to be low.	<i>(no explanation returned by the model)</i>
11	Given that the severity of the COVID-19 pandemic is low and the potential end of the pandemic is false, there would be no severe travel restrictions imposed worldwide. The low severity of the pandemic suggests minimal disruption, and since there’s no potential end of the pandemic yet, current measures would likely remain in place but not be stringent.	Given that the severity of COVID-19 pandemic is low and there is a potential end of COVID-19 pandemic, it can be inferred that travel restrictions imposed worldwide would likely be none. This is because a low severity of the pandemic suggests that the situation is under control, and a potential end to the pandemic would further reduce the need for travel restrictions.
12	Since the travel restrictions imposed worldwide were 'none' yesterday, it is likely that the oil & gas and airlines sectors condition was 'good'. Severe travel restrictions would worsen these sectors, but in the absence of any restrictions, the condition should be favorable.	Given that yesterday there were no worldwide travel restrictions, it is estimated that the condition of oil & gas and airlines sectors was good.
h0	The value cannot be determined as there are no parent causes provided to infer the outcome.	The potential end of COVID-19 pandemic will occur because all the parent causes have values that lead to this outcome.

1080
1081
1082
1083
1084
1085
1086
1087
1088
1089
1090
1091
1092
1093
1094
1095
1096
1097
1098
1099
1100
1101
1102
1103
1104
1105
1106
1107
1108
1109
1110
1111
1112
1113
1114
1115
1116
1117
1118
1119
1120
1121
1122
1123
1124
1125
1126
1127
1128
1129
1130
1131
1132
1133

Table 7: Example of graph scores explanations given by GPT-4o in Table 5. FG stands for Factual Graph and CG for Counterfactual Graph. Sc stands for Score and Cf stands for confidence. We show the explanations for one graph and two counterfactual graphs.

	Sc	Cf	GPT-4o
FG	0.85	0.85	The sequence of events and their causal relationships are highly plausible given the context of the COVID-19 pandemic and global economic conditions. The COVID-19 pandemic had a significant impact on global markets, including Bursa Malaysia, leading to a downtrend in FBM KLCI points. The severity of the oil price war also contributed to this downtrend. Travel restrictions due to the pandemic affected both the oil and gas sector and the airline sector, leading to further economic pressure. The change in Malaysia’s coalition government affected corporate earnings, contributing to the overall economic situation. The lack of financial support from the government increased pressure on bank stocks, especially given the bad operating conditions for SMEs. The values provided for FBM KLCI points and other financial metrics are consistent with the described events and their causal relationships. Therefore, the overall sequence of events is highly plausible.
CG1	0.5	0.5	Let’s break down the events and their causal relationships one by one: 1. Travel restrictions (Event 0) are false, meaning there are no travel restrictions in place. 2. The severity of the oil price war (Event 1) is high, which indicates a significant conflict impacting oil prices. 3. The severity of the COVID-19 pandemic (Event 2) is also high, suggesting widespread impact from the pandemic. 4. Travel restrictions affect the oil and gas sector condition (causal relationship 0 -> 3). 5. The condition of the oil and gas sector (Event 3) is bad. Given the provided events and relationships, the key causal link to evaluate is between travel restrictions (Event 0) and the oil and gas sector condition (Event 3). Since travel restrictions are not in place (false), this would typically suggest a neutral or positive impact on the oil and gas sector. However, the sector condition is bad. This could be due to other factors not explicitly mentioned in the graph, such as the high severity of the oil price war (Event 1) and the high severity of the COVID-19 pandemic (Event 2). The graph doesn’t explicitly link these other factors to the oil and gas sector condition, but they are plausible contributors. Overall, the sequence of events seems somewhat plausible but lacks explicit causal links for all influencing factors, resulting in a moderate score and confidence.
CG2	0.3	0.5	The causal graph has several issues that impact its overall plausibility. First, the event ‘FBM KLCI earnings decline in 2009’ is given a value of 5.0, which is plausible given the historical context of the 2008-2009 financial crisis. However, the subsequent events ‘Severity of COVID-19 pandemic’ and ‘Severity of oil price war’ are not assigned values, making it difficult to evaluate their plausibility. The link between ‘FBM KLCI earnings decline in 2009’ and ‘Potential earning downside risk’ is plausible, as past earnings declines can influence future downside risks. However, the lack of values for the severity of the pandemic and oil price war significantly reduces the confidence in the overall plausibility of the causal graph.

1134
 1135
 1136
 1137
 1138
 1139
 1140
 1141
 1142
 1143
 1144
 1145
 1146
 1147
 1148
 1149
 1150
 1151
 1152
 1153
 1154
 1155
 1156
 1157
 1158
 1159
 1160
 1161
 1162
 1163
 1164
 1165
 1166
 1167
 1168
 1169
 1170
 1171
 1172
 1173
 1174
 1175
 1176
 1177
 1178
 1179
 1180
 1181
 1182
 1183
 1184
 1185
 1186
 1187

Table 8: Example of graph scores explanations given by LLaMA3.1 in Table 5. FG stands for Factual Graph and CG for Counterfactual Graph. Sc stands for Score and Cf stands for confidence. We show the explanations for one graph and two counterfactual graphs.

	Sc	Cf	LLaMA-3.1
FG	0.7	0.8	The plausibility of the sequence of events is high due to the following reasons: COVID-19 pandemic (event 0) has a direct impact on recessionary trends (event 1). Fiscal policy responses (event 2) mitigated the effects of recessionary trends. However, oil price war (event 3) influenced FBM KLCI (event 4), which was also impacted by COVID-19 pandemic and recessionary trends.
CG1	0.6	0.7	The event 'COVID-19 pandemic' with a value of True increases the likelihood of recessionary trends and has an impact on FBM KLCI. The event 'Oil price war' with a value of 80 influences FBM KLCI but is not directly linked to recessionary trends, despite its potential indirect impact. However, recessionary trends are False which decreases the likelihood of FBM KLCI being influenced by it.
CG2	0.0	0.8	The COVID-19 pandemic has had a significant impact on the global economy, leading to recessionary trends. However, fiscal policy responses have mitigated some of these effects. The oil price war has also influenced the FBM KLCI, but its overall value remains high.